AIAA 2002-0310

ETW ANALYTICAL APPROACH TO ASSESS THE WING TWIST OF PRESSURE PLOTTED WIND TUNNEL MODELS

Norbert Gross*
European Transonic Windtunnel
Ernst-Mach-Strasse
D-51147 Köln
Germany

Abstract

Exploiting the unique ability of the European Transonic Windtunnel to vary the free-stream dynamic pressure at constant Reynolds number (and vice versa), the effective aerodynamic wing twist is determined by comparing the normalized pressures measured at certain wing sections. This task is performed by a computer program which processes the pressures of one individual wing section that have been acquired at the same Mach and Reynolds number, but different levels of tunnel pressure and temperature, i.e. different dynamic pressures. To obtain the geometric twist, the induced downwash angle which originates from the effective wing twist alone is estimated and added to the effective wing twist.

This paper describes the effect of the wing twist on the measurement results, the mathematical model used to determine the effective aerodynamic twist and the features of the above mentioned software. The relationship between wing bending and twist in the case of a swept wing and its impact on the results is discussed as well as the computation of the geometric wing twist. The last section contains an assessment of the accuracy and the description of the advantages and disadvantages of the presented method.

List of Symbols

a_0, a_1	polynomial coefficients
b	half wing span
$c(\eta)$	local chord length
c	mean aerodynamic chord
C_L	lift coefficient
$C'_{L\infty}$	$dC_L/d\alpha$ of an infinitely long wing
C_p	pressure coefficient
E	modulus of elasticity
L	lift force
M	Mach number
q	free-stream dynamic pressure
Re	chord Reynolds number
α	model angle of incidence
γ	normalized circulation
$\varepsilon(\eta)$	local wing twist
η	relative wing span ($-1 \le \eta \le 1$)

Introduction

For a few years now cryogenic wind tunnels are able to test aircraft models at high Reynolds numbers, requiring an elevated tunnel pressure with a corresponding increase in the aerodynamic loads and therefore in the elastic deformation of the wing†. Although the independent variation of Reynolds number (at constant q/E) and dynamic pressure (at constant Re) allows the separate evaluation of the resulting effects, the respective shape of the wing, especially its twist, is essential information for the development engineer.

Based on the assumption that each tap on a pressure plotted wing located in an area where the local pressure shows a distinct variation with the angle of attack can be regarded as a pitch meter, the local effective wing twist can be computed and the approximate geometric twist estimated.

Effect of the Wing Twist on Test Results

In the case of ETW as a cryogenic facility the client has not only to make up his mind at which Reynolds number he wants to perform a test, but has also to decide on tunnel pressure and temperature. As shown in Figure 1, the same Reynolds number can be achieved at a variety of pressure and temperature combinations, each resulting in a different dynamic pressure and therefore different model loads, deformations and finally test results.

* Data Reduction Engineer

† For example, the lift produced by a suitably scaled transport aircraft model at cruising speed and flight Reynolds number can easily reach 20 kN, leading to a local wing twist near the tip of more than 2° for a model made of steel.

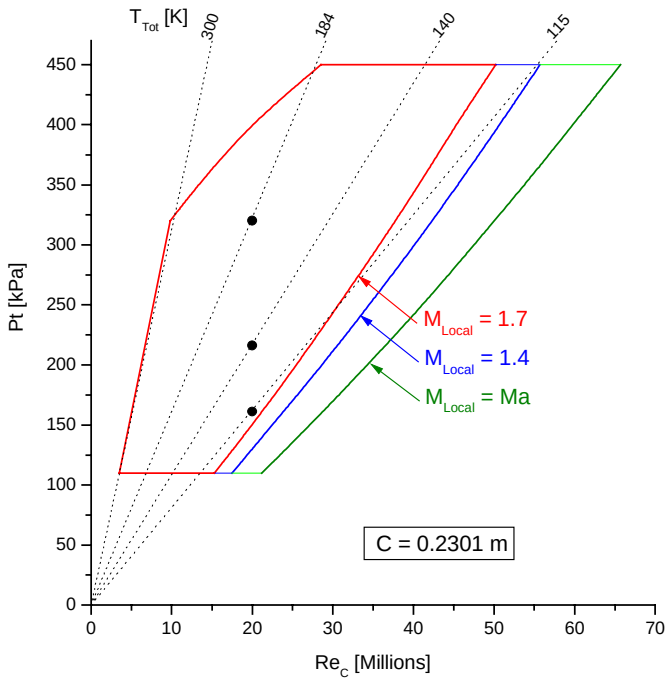

Figure 1: ETW Envelope at M=0.85, c=0.2301 m

The effect of the wing twist on the lift coefficient is shown in Figure 2, the effect on the axial force coefficient in Figure 3, with the model and test conditions being those of Figure 1. Lift and axial force are clearly decreasing with increasing tunnel pressure, in the case of the axial force distinctly more than the aspired 1 drag count accuracy.

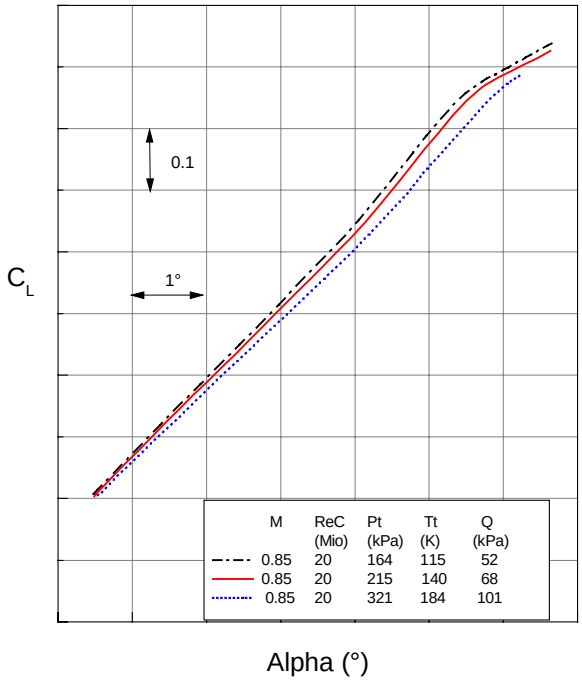

Figure 2: Effect of the wing twist on the lift force at constant Reynolds number.

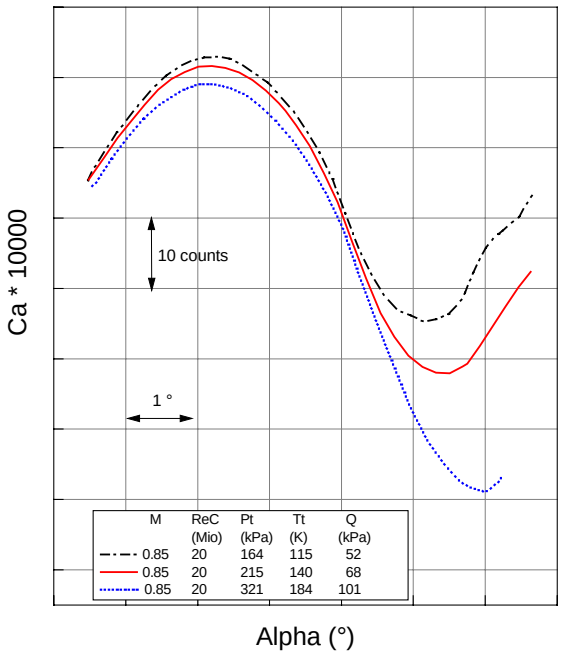

Figure 3: Effect of the wing twist on the axial force at constant Reynolds number.

Depicted in Figure 4 are the pressure distributions measured at 7 wing sections at about the same angle of incidence, the one in the lower left corner being close to the fuselage. As one expects, the differences are very small at the inner part of the wing and are considerably increasing towards the wing tip. Although all relevant test conditions (M, Re and α) have been kept constant, in fact one parameter, i.e. the wing deformation, has been involuntarily varied, thus raising the question "which model has been actually tested".

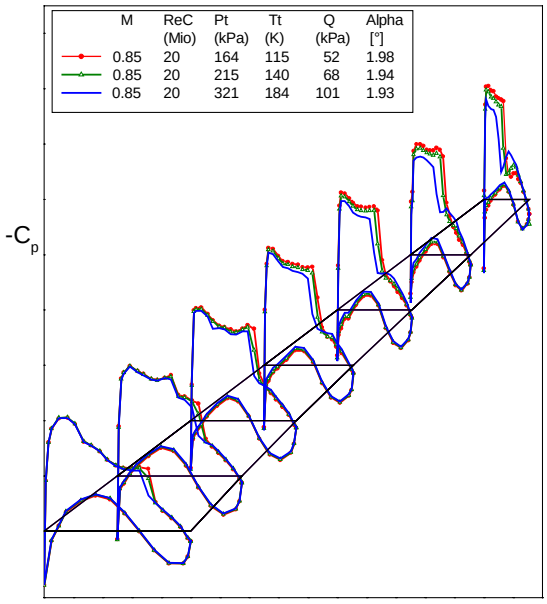

Figure 4: Effect of the wing twist on the local pressure distribution at constant Reynolds number.

Determination of the Effective Wing Twist

The basic idea of the ETW approach is to view each wing section individually: the two most similar pressure distributions in the data of two polars, which were taken at the same Mach and Reynolds number, but different levels of the dynamic pressure, are interpreted as representing the same local effective angle of attack, and the α difference is regarded as the difference in the local effective wing twist. Writing this as a mathematical equation (indices 1 and 2 representing different q levels), we get

$$\alpha_{local} - \alpha_{model,2} - (\alpha_{local} - \alpha_{model,1}) = \varepsilon_{eff,2} - \varepsilon_{eff,1}$$

and after eliminating the unknown local α

$$\alpha_{model,2} - \alpha_{model,1} = -(\varepsilon_{eff,2} - \varepsilon_{eff,1}) \qquad (1)$$

The following simple mathematical model has been chosen to describe the effective twist as a linear function of dynamic pressure and lift force:

$$\varepsilon_{eff} = f(q,L)$$

or after substituting L by $C_L \times q$:

$$\varepsilon_{eff} = -(a_0 + a_1 \times C_L) \times q \qquad (2)$$

The final equation is obtained by combining Equations (1) and (2), assuming that $C_{L,1} \approx C_{L,2}$:

$$\frac{\alpha_{model,2} - \alpha_{model,1}}{q_2 - q_1} = a_0 + a_1 \times C_L \qquad (3)$$

which contains no unknowns besides coefficients a_0, a_1 and can be solved by applying a least square fit to the pairs of variates $C_L, \Delta\alpha/\Delta q$ obtained from the comparison of the pressure distributions at different values of C_L.

However the initial idea of comparing the shape of the pressure distributions at individual wing sections turned out to give inaccurate results due to the fact that the flow is considerably deflected on its way from the leading to the trailing edge. Therefore in a second approach the pressure taps were regarded as individual pitch meters (Figure 5), and the $\Delta\alpha$ at a given angle of incidence determined separately for each tap of the processed wing section. This means that Equation (3) describes in fact a linear transformation from the model to the local coordinate system, thus mapping the measured α, C_p curves shown in Figure 5 upon each other.

This second approach has the advantage of better robustness and allows in addition the reduction of the number of pressure taps required to evaluate the local effective wing twist to about 4-5. Although the problem of the deflected flow per se is not solved, it can be coped with by using only those taps which are located in a mainly unaffected area. If this is not possible, the results can be approximately corrected if the deflection angles are known from CFD calculations (a more detailed discussion follows in the next paragraph).

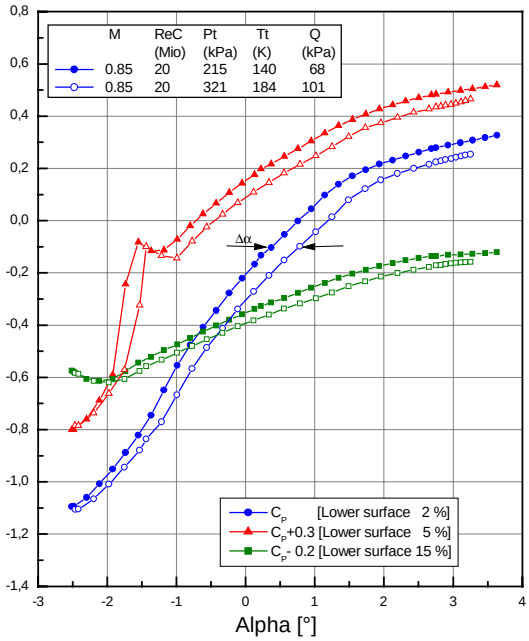

Figure 5: Pressure coefficients of selected taps as function of the incidence angle at the outboard section η=0.84

The software which has been developed to determine the coefficients a_0, a_1 of Equation (3) performs the following steps [2]:

- Input of the data of 2 to 3 polars belonging to one wing section and interpolation in steps of 0.15°
- Computation and assessment of the ratio $\Delta\alpha_i/\Delta q$ for all taps and all α_i, including:
  - Elimination of invalid or nearly constant pressure data.
  - Weighting of all $\Delta\alpha_i/\Delta q$ values with the local pressure gradient $dC_{p,i}/d\alpha_i$.
  - Successive exclusion of those $\Delta\alpha_i/\Delta q$ values which by a certain amount exceed the regression value that has been computed for the current incidence angle $\Delta\alpha_i$.
  - Determination of a possible offset ΔC_p caused by temperature drift or inaccuracies in the in-situ calibration* of the pressure scanners.
  - Complete re-computation of all $\Delta\alpha_i/\Delta q$ values with ΔC_p applied.

* Performed prior to any test run.

- Computation of the coefficients a_0 and a_1 via linear regression.
- Opening of a window on the terminal screen displaying the diagram C_L,$\Delta\alpha/\Delta q$, in addition offering the possibility to interactively eliminate obvious outliers by pointing at the respective marker and pressing Mouse Button 1.
- Storage and printing of the manually performed modifications.

The results obtained at two wing sections are presented in Figures 6 and 7. Deactivated outliers are immediately excluded from the regression analysis, but remain visible for documentation purposes[†].

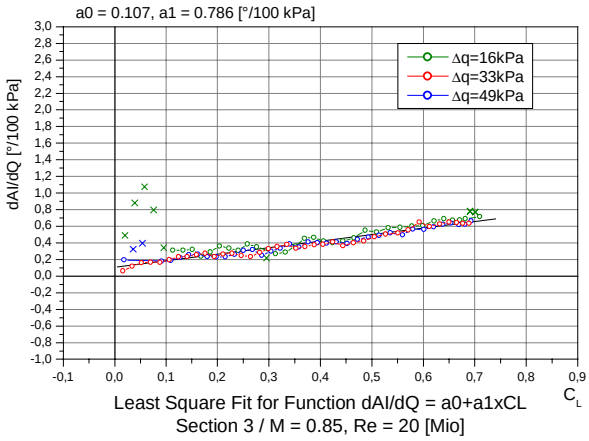

Figure 6: Evaluation of the wing pressures of a full model at η=0.47

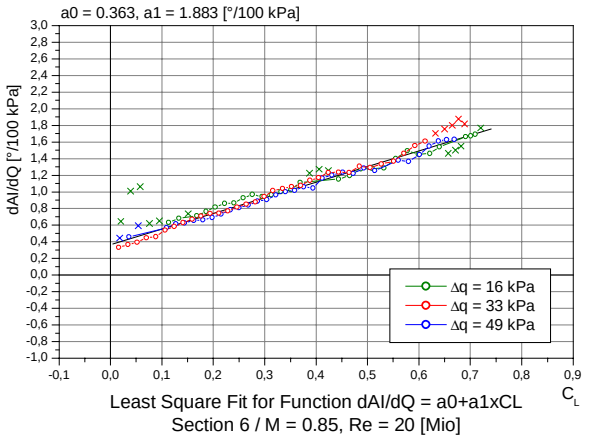

Figure 7: Evaluation of the wing pressures of a full model at η=0.84

The scaling of the ordinate in °/100 kPa has been chosen because 100 kPa represent a typical value of the dynamic pressure at high Reynolds number tests, and the fixed scaling allows the direct comparison and assessment of the data scatter.

A number of important conclusions can be drawn from Figures 6 and 7:

- The results of the analysis are independent of Δq (the high Δq exceeds the low Δq by a factor of 3).
- The effective wing twist does not become zero at C_L=0 because of the pitching moment being ≠0.
- The C_L, $\Delta\alpha/\Delta q$ graph remains linear even at high incidence angles where the slope of the α,C_L graph is significantly reduced.
- The assumption of the local effective twist being a linear function of dynamic pressure and lift force (Equation (2)) has been confirmed (at least for this type of model).

Figure 8 shows the graphs of Figure 5 with the linear transformation $\Delta\alpha = (a_0 + a_1 \times C_L) \times \Delta q$ applied to the high pressure data. Although areas with relatively high deviations exist, these are identified by the software and automatically excluded from the evaluation, which demonstrates the robustness of the process.

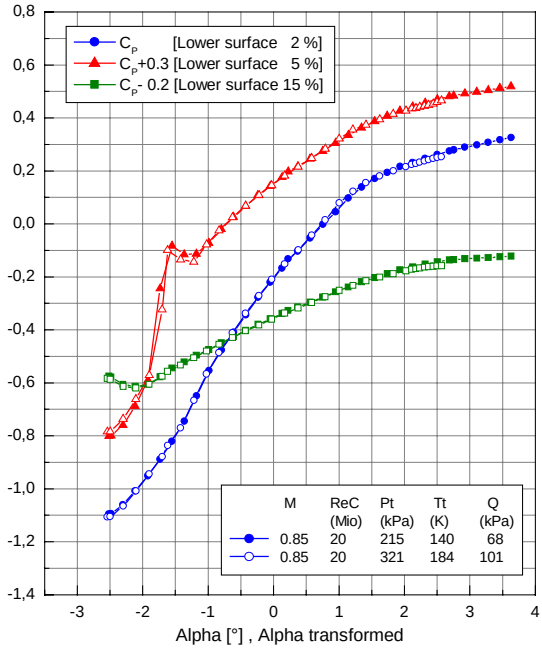

Figure 8: Pressure coefficients of selected taps as function of the angle of incidence at the outboard section η=0.84, α transformation applied to high pressure data.

[†] Reactivation via Mouse Button 2 is also possible.

The effective twist at 6 different values of C_L, obtained from the data of 7 wing sections, has been plotted vs. relative wing span in Figure 9. The wing root is located at $\eta \approx 0.11$, and the trailing edge kink at $\eta \approx 0.34$. The obvious dependence of the wing twist on the lift is discussed in the next paragraph, the relationship between effective and geometric twist (shown as dashed line) in the paragraph after.

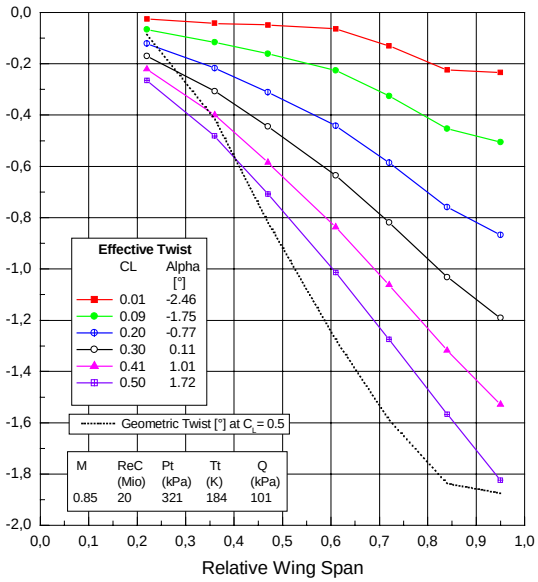

Figure 9: Results of a complete wing twist analysis: Effective twist vs. wing span. Estimated geometric twist (C_L=0.5) shown as dashed line.

Bending and Twist of a Swept Wing

A particular feature of swept wings is the aerodynamic twist due to bending as shown in Figure 10. Although a pure bending along the centre line has been simulated, an increasing negative twist angle[‡] towards the wing tip is observed. This explains the above postulated and later on confirmed linear relationship between local twist and lift.

The coupling between wing bending and twist[§] is also the reason for the above mentioned inaccuracy if the flow deviation on the upper and lower surface is not taken into account. A deviation towards the fuselage has the same effect as reducing the sweep angle and hence the twist due to bending, which means that the pitch meter (i.e. wing pressure tap) measures a local twist which is too low. The opposite holds true if the flow is deflected towards the wing tip. It is therefore desirable to have access to streamline plots from CFD calculations to be able to either select pressure taps which are located in a region with negligible flow deviations[**], or to apply approximate corrections to the results making use of the known deflection angles.

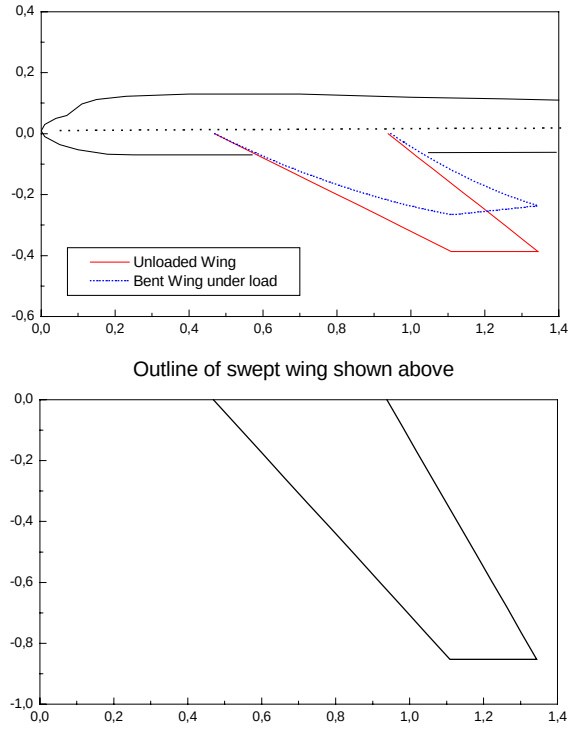

Figure 10: Aerodynamic twist of a swept wing due to pure bending.

Estimate of the Geometric Wing Twist

According to classical lifting surface theory, the vortex system generated by the wing induces a downwash, resulting in a reduced angle of attack called the true (or effective) angle of incidence:

$$\alpha_{true} = \alpha_{geometric} - \alpha_{induced}$$

Figure 11 shows how this affects the untwisted and the twisted wing: in both cases the wing tip is attacked by the flow under the same effective angle α_e (found by comparing the local pressures), however because of the stronger downwash produced by the untwisted wing, this can only be achieved if the geometrical angle of incidence of the untwisted wing is greater than that of the twisted wing.

‡ Bending of a forward swept wing results in a positive wing twist.

§ For small bending angles < 5°, the local twist angle due to bending can be calculated as:
$\varepsilon_b = \text{atan}(\sin\gamma \times \tan\beta)$, γ: sweep back angle, β: local bending angle

** e.g. between 1 and 50% chord length on the lower surface

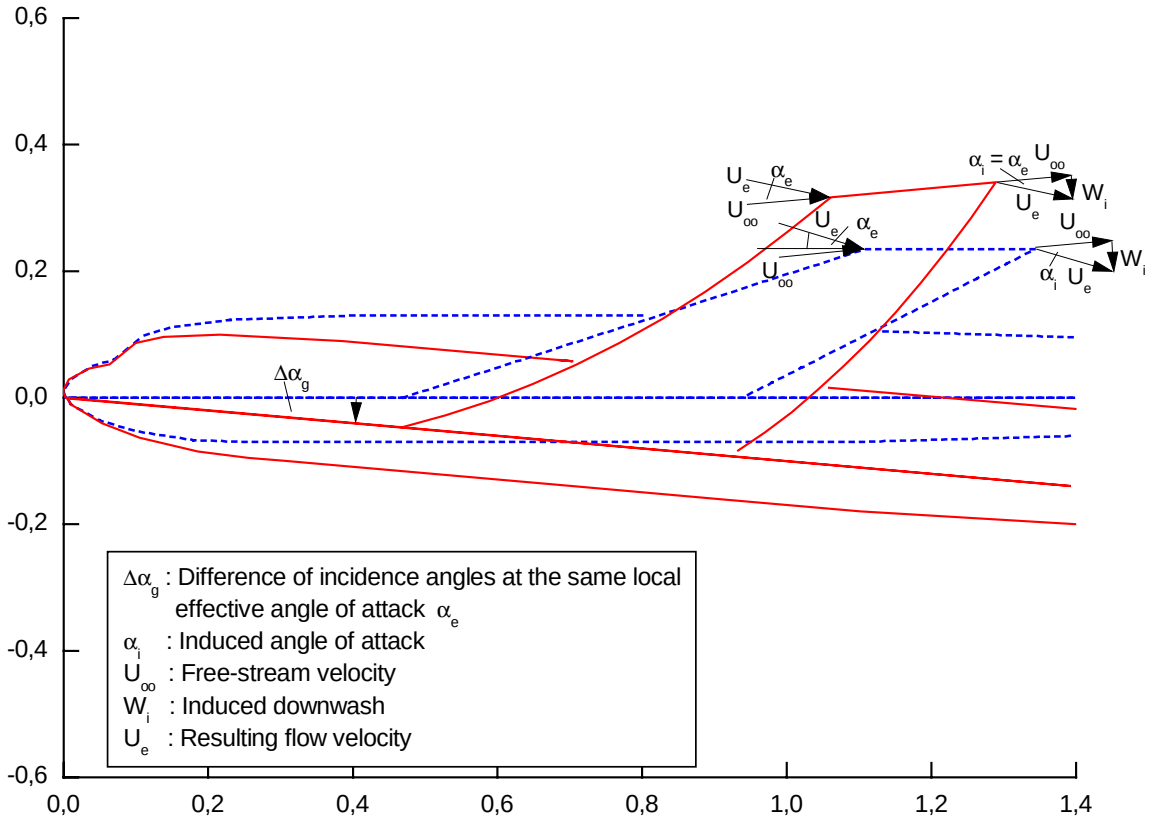

Figure 11: Effect of the induced downwash on the local angle of attack for a twisted and an untwisted wing.

The difference in the incidence angles $\Delta\alpha_g$ is therefore lower than the difference in the local geometric wing twists. The latter can nevertheless be assessed by adding the induced downwash, which is due to the wing twist alone, to the local effective twist obtained from Equation (2):

$$\varepsilon_{geometric}(\eta) = \varepsilon_{eff}(\eta) + \Delta\alpha_{induced}(\eta) \qquad (4)$$

To validate what has been said above, the induced downwash of an untwisted and a twisted wing have been computed by solving the downwash integral of the lifting line theory, assuming an elliptical distribution of the circulation at C_L=0.5 in the case of the untwisted wing. The result is shown in Figure 12: in accordance with theory the untwisted wing produces a constant downwash, whereas the downwash of the twisted wing[††] is higher at the inner and lower at the outer part of the wing. This also explains the fact that the characteristics in Figure 9 depicting the effective and the geometric twist at C_L=0.5 intersect at η=0.4.

To obtain the induced angle of incidence required to assess the geometric wing twist (Equation 4), the normalized circulation γ is computed according to [1]:

$$\gamma(\eta) = C'_{L\infty} \times \varepsilon_{eff}(\eta) \times c(\eta) / 2b \qquad (5)$$

The local effective wing twist ε_{eff} is described by Equation 2, local chord length c(η) and half wing span b are known from the wing geometry. If the slope $dC_L/d\alpha$ of the α,C_L curve of the infinitely long wing, i.e. the profile characteristic $C'_{L\infty}(\eta)$, is either known from CFD calculations or estimated from the test results, the derivative dγ/dη can be calculated and the downwash integral[‡‡]

$$\alpha_i(\eta) = \frac{1}{2\pi}\int_{-1}^{+1}\frac{d\gamma}{d\eta'}\frac{d\eta'}{\eta-\eta'}$$

solved for one combination of M, Re, q and C_L at a time.

[††] A twist which is parabolically increasing towards the wing tip has been simulated.

[‡‡] Two interesting aspects of the downwash integral are:

- The induced downwash is not determined by the magnitude of the circulation, but by its gradient. This means that an infinitely long wing produces no downwash and has therefore no induced drag.
- Due to the hyperbolic character of the integration function the downwash is dominated by the gradient of the circulation in its close vicinity, although the integration interval spans the complete wing.

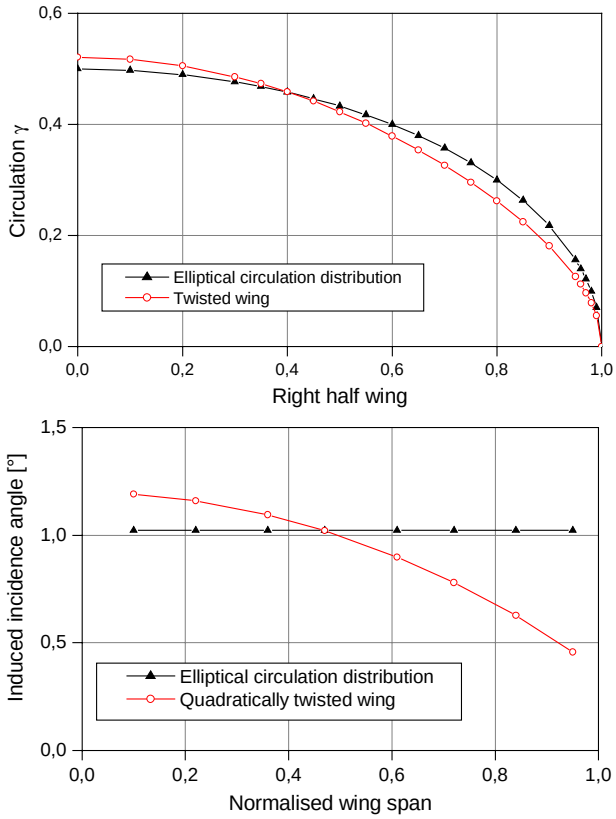

Figure 12: Circulation distribution and induced incidence angle of a twisted and an untwisted wing

Assessment of the Method

Since no reference data is available and a validation in the laboratory is not possible, the accuracy of the ETW approach to assess the wing twist for pressure plotted models can only be estimated. From Figures 6, 7 and 13 it can however be concluded that - good data quality provided - low data scatter and an excellent resolution of even very small differences in the local twist (Figure 13) are achievable. Based on the experience that has been gained with different models, an uncertainty in the results of the wing pressure evaluation of about ±0.1° seems to be a realistic assumption. The additional uncertainty which is due to the deflection of the streamlines and the induced downwash depends mainly on the quality and extent of the information provided by the client.

The main disadvantages of the method are:

- Requires a pressure plotted wind tunnel model (however the measurement method is in principle not limited to pressure taps, e.g. pressure data of comparable accuracy originating from tests with pressure sensitive paint are suitable as well).

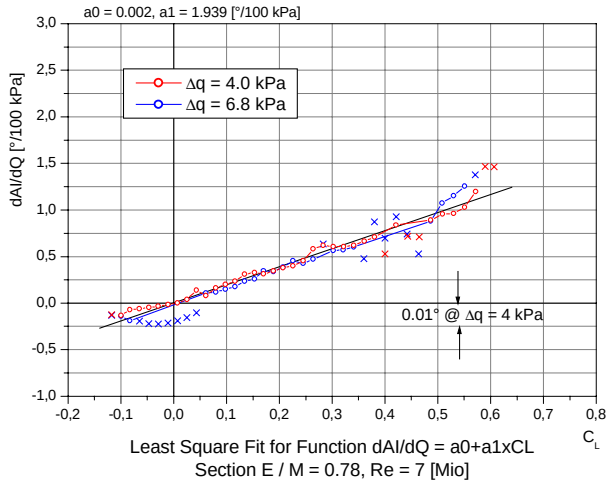

Figure 13: Evaluation of the wing pressures of a half model at η=0.85

- Allows no reliable prediction of the achievable accuracy prior to the availability of measurement data.
- If the geometric twist is to be determined by ETW, the accuracy will be reduced due to the uncertainty in the assessment of the induced downwash.

The main advantages of the method are:

- Usable over the full operating range of the tunnel.
- Based on a well proven measurement technique.
- Requires neither surface treatment (e.g. coating) nor additional instrumentation or calibration.
- Model attitude and mounting have no effect on applicability and accuracy (can be used for full and half models).
- Insensitive to vibrations, turbulence, temperature gradients, etc.
- Simple computation of the effective twist for all values of C_L and q.

Conclusion

In the case of pressure plotted wind tunnel models the approach presented in this paper offers the opportunity to assess the local wing twist with nearly no additional expense. It thereby represents at least a welcome supplement to other methods, in certain cases it might even be considered a true alternative.

To take full advantage of its potential and to improve the accuracy particularly in calculating the induced downwash, beside the gathering of further experience the cooperation of the client in providing the results of CFD computations as well as feed-back information is required.

References

[1] **Schlichting, H., Truckenbrodt, E.**
Aerodynamik des Flugzeuges, Zweiter Band, Springer-Verlag Berlin, 1969

[2] **Gross, N.**
Determination of the Effective Aerodynamic Twist by Comparison of Wing Pressures, Technical Memorandum ETW/TM00.033 (2000)